Catalysis Science & Technology

ROYAL SOCIETY OF CHEMISTRY

PAPER

View Article Online
View Journal | View Issue

Cite this: *Catal. Sci. Technol.*, 2021, 11, 7886

Continuous enzymatic stirred tank reactor cascade with unconventional medium yielding high concentrations of (*S*)-2-hydroxyphenyl propanone and its derivatives†

Reinhard Oeggl,[ab] Juliane Glaser,[ac] Eric von Lieres [a] and Dörte Rother *[ab]

The implementation of biocatalysis in flow chemistry offers synergistic synthesis advantages in line with green chemistry principles. Yet, the conversion of high substrate concentrations is in many cases hindered by insolubility issues or substrate toxicity. Here, the continuous synthesis of (*S*)-2-hydroxyphenyl propanone (2-HPP) from inexpensive benzaldehyde and acetaldehyde in a methyl *tert*-butyl ether based organic reaction environment, namely micro-aqueous reaction system, has been established. Kinetic parameters of the applied whole cell catalyst were identified to design a continuous process for (*S*)-2-HPP synthesis. This revealed a necessity to distribute acetaldehyde over a spatial coordinate to remain below a toxic concentration threshold. Hence, three continuous stirred tank reactors (cSTR) were conjugated in a technical cascade with an additional influx of acetaldehyde into each unit. The catalytic behaviour of this reaction setup was described based on mass balances and a kinetic model. Enzyme deactivation was described by a novel staged model and compared to a simple generic model. The optimized continuous setup yielded 190 mM (*S*)-HPP with an ee > 98% over 8 h. The product was easily recovered from the organic reaction environment by crystallization with an isolated yield of 68% and a purity of >99%. Further, the substrate range of the applied catalyst *Pseudomonas putida* benzoylformate decarboxylase variant L461A was analysed. This revealed numerous halogenated, methoxylated and nitro-derivatives in *ortho*, *meta*, and *para* position, which can in principle be gained by the established process. As an example, the applied cSTR concept was transferred to *p*-methoxy benzaldehyde with good results even without further optimization.

Received 24th August 2020,
Accepted 13th September 2021

DOI: 10.1039/d0cy01666g

rsc.li/catalysis

Introduction

In recent years continuous flow chemistry utilizing biocatalysis has emerged as a promising tool to fulfil the goal of sustainable fine chemical synthesis in the aspects of green chemistry.[1,2] A notable difference of flow chemistry with biocatalysts compared to organic synthesis is that predominantly buffered systems are used for catalytic reactions.[3] Unfortunately, many substrates leading to valuable compounds suffer from poor substrate solubility and thereby poor overall synthesis efficiency.[4,5] Furthermore, also soluble concentrations of substrate may lead to toxic effects on biocatalysts and deactivate them. For instance, the synthesis of (*S*)-2-hydroxy-1-phenylpropanone ((*S*)-2-HPP) from acetaldehyde and benzaldehyde in buffered systems is firstly limited by the poor solubility of benzaldehyde in buffered systems, which does not exceed 40 mM. Secondly, the highly reactive substrate acetaldehyde is known to deactivate the biocatalyst catalysing the reaction.[6,7]

Herein, we aim to overcome these challenges and establish a continuous production process for high (*S*)-2-HPP concentrations in a hydrophobic reaction environment. The process development in the ideal biocatalytic operation window of high substrate concentration while dealing with substrate toxicity will be supported by descriptive reaction models of different complexities. Further, an extended usability of biocatalytic operations in hydrophobic reaction environments is targeted by demonstrating a simple product isolation procedure and a process transfer to a product platform of derivatives.

The stereo- and chemoselective synthesis of (*S*)-2-HPP from benzaldehyde and acetaldehyde is so far only described by the *Pseudomonas putida* benzoylformate decarboxylase (*Pp*BFD), a thiamine-dependent carboligase.[8] An advantage is

[a] *IBG-1: Biotechnology, Forschungszentrum Jülich GmbH, 52425 Jülich, Germany. E-mail: do.rother@fz-juelich.de*
[b] *Aachen Biology and Biotechnology (ABBt), RWTH Aachen University, 52074 Aachen, Germany*
[c] *Digital Integration & Predictive Technologies (DIPT), Amgen Research (Munich) GmbH, Staffelseestr. 2, 81477 Munich, Germany*

† Electronic supplementary information (ESI) available. See DOI: 10.1039/d0cy01666g

that the most selective enantioselective *Pp*BFD variant L461A meets the enantiopurity required for fine chemicals by achieving a remarkable ee of 98% for (*S*)-2-HPP (Fig. 1).[8,9] Nonetheless, this variant, as well as many ligases applied for 2-hydroxy ketone synthesis, suffer from acetaldehyde sensitivity and poor benzaldehyde solubility.[10–17]

The challenge of benzaldehyde solubility was recently mastered in batch applications by applying a moisture controlled micro-aqueous reaction system (MARS).[6,7,17–20] MARS provides solvent sensitive enzymes with a stable monophasic environment to react in hydrophobic solvent solutions. This system is obtained by suspending a lyophilized whole cell (LWC) catalyst in pure substrate solutions or substrate/solvent mixtures and adding a minor buffer fraction.[18,19] The buffer fraction should not exceed the solubility limit. The expression levels of recombinant *Pp*BFD varL461A in the LWCs are elevated to such an extent that background reactions are rendered negligible.[6,7,17,19,21] The potential of this unconventional reaction medium in batch synthesis for (*S*)-2-HPP production was successfully demonstrated by Wachtmeister *et al.*, by obtaining 340 mM product with an ee of 98%.[17] The promising results of other MARS batch applications further encourage an exploration of its potential in continuous operation to achieve synthesis at high substrate concentrations.[6,7,19]

While a MARS elevates the limits of benzaldehyde solubility, the challenge of enzyme deactivation by acetaldehyde persists. To utilize the high concentrations possible in MARS, acetaldehyde has to be added in smaller portions. In classic continuous syntheses this is realized with a continuous cross flow reactor (Fig. 2A), which allows the distribution of acetaldehyde over the whole column length. For practical reasons in the herein performed process development, this setup is emulated by setting up a continuous stirred tank reactor cascade (cSTR-c; Fig. 2B). This allows a distribution of the total acetaldehyde amount over the respective cSTR-c units and thereby keeping local substrate concentration below a level that would trigger an accelerated enzyme deactivation.

The molecular reactions inside the cSTR-c with biocatalytic synthesis and simultaneous enzyme deactivation are poorly understood. Mechanistic models are a powerful tool to gain a better understanding already from small data sets. Here, a simplified mechanistic model is developed for process analysis and optimization. The reactor model relates

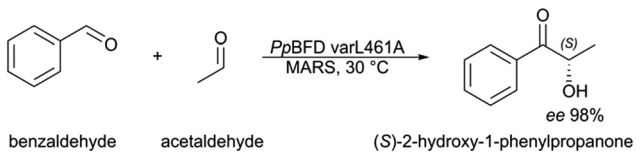

Fig. 1 Synthesis of (*S*)-2-hydroxy-1-phenylpropanone. Benzaldehyde and acetaldehyde are ligated to the chiral (*S*)-2-hydroxy ketone by *Pseudomonas putida* benzoylformate decarboxylase variant L461A in a micro-aqueous reaction system (MARS).

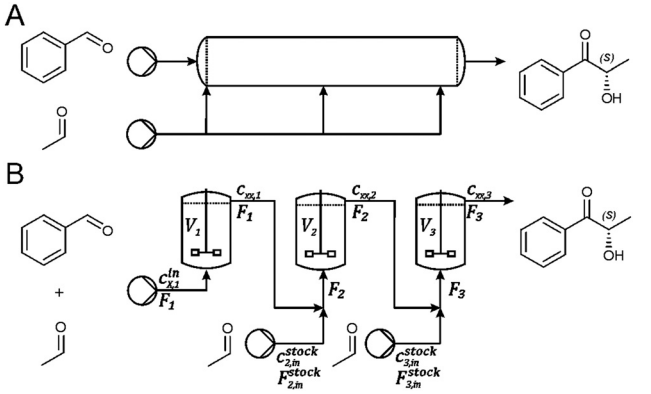

Fig. 2 Methods to minimize effects of substrate toxicity in continuous processes. (A) A continuous cross flow reactor is a suitable method to distribute the total substrate amount, in this case acetaldehyde, over the length of the column avoiding toxification by substrates. In lab-scale such a setup is emulated by (B) a continuous stirred tank reactor cascade (cSTR-cascade). In this manner high concentration of continuously synthesized (*S*)-2-HPP can be gained, while reducing effects of substrate toxicity to a minimum. This is done by controlling influx flow rates F_i [m^3 s^{-1}] and the addition of acetaldehyde c_i [mM] ($i \in \{2, 3\}$) in the defined constant reactor volume V [m^3].

the concentration changes of reactants upon enzymatic conversion in the respective unit of the cSTR-cascade to a mass balance of fluxes into and out of that cSTR-c unit. The catalyst is modelled by a 2nd order Michaelis–Menten kinetic with reversible inhibition by acetaldehyde and additional acetaldehyde concentration-dependent enzyme deactivation. The model is calibrated using measurement data in order to predict substrate turnover rates, (*S*)-2-HPP conversion, and stable operation time to achieve a stable product output in the cSTR-cascade.

The gained product is easily isolated by utilizing the benefits of MARS.[6,7,17–19] The recently demonstrated direct product crystallization from the reaction solution, which is facilitated by the well distinguished physicochemical properties of all reactants in MARS, is intruguing.[6]

To extend the applicability of the presented process, the substrate range of *Pp*BFD varL461A is analysed with respect to halogenated, methoxylated and nitro-benzaldehyde derivatives. As proof of concept, the *p*-methoxy benzaldehyde derivative is used without further parameter optimization in the cSTR-cascade to prove the general applicability for the synthesis of (*S*)-2-HPP derivatives in the outlined manner.

Methods and materials

Materials

Chemicals. Acetaldehyde, benzaldehyde and benzaldehyde derivatives were purchased from Sigma Aldrich with purities ≥98% and handled under argon atmosphere. Anhydrous methyl *tert*-butyl ether (MTBE) was obtained from Alfa Aesar with purities ≥98%. Triethylamine (TEA), $MgSO_4$, and

thiamine-diphosphate (ThDP) were purchased from Sigma Aldrich in purities ≥99%. 2-Propanol and *n*-heptane were supplied by Biosolve Chimie SARL in HPLC grade. Both enantiomers of 2-hydroxy-phenylpropanone (2-HPP) and derivatives thereof were synthesized enzymatically and purified under the same conditions as described by Jakoblinnert and Rother.[7]

Enzyme preparation. In all experiments *Pp*BFD varL461A (protein sequence see PDB 2V3W) was formulated as lyophilized whole cell (LWC) catalyst. Therefore, *Pp*BFD varL461A was heterologously produced in *Escherichia coli* BL21 in a high cell density cultivation as described by Gocke.[8] Cells were harvested by centrifugation at 4000 rcf and 4 °C. The cell pellet was frozen at −20 °C and then lyophilized at −54 °C and <0.010 bar. LWCs were mortared and stored at −20 °C upon usage.

Methods

In the following the term conversion is defined as the percentage share of benzaldehyde or benzaldehyde derivative that has been carboligated with acetaldehyde to the desired 2-HPP product by mass balancing the measured aromats benzaldehyde and (*S*)-2-HPP.

Reaction kinetic of *Pp*BFD varL461A for the synthesis of (*S*)-HPP in MARS. Specific initial activities of *Pp*BFD varL461A LWCs were recorded in batch to determine kinetic parameters. Specific initial activity is defined as a catalytic activity achieved below 10% conversion. Therefore, an orthogonal substrate concentration array of acetaldehyde concentrations between 25 mM to 200 mM and benzaldehyde concentrations between 50 mM to 300 mM were prepared in MTBE. The respective substrate solution was added to 20 mg mL^{-1} *Pp*BFD varL461A LWCs. Reactions were started by adding 20 μL mL^{-1} 1 M triethylamine (TEA) buffer pH 10 with 5 mM thiamine diphosphate (ThDP) and 25 mM magnesium sulphate ($MgSO_4$) and subsequently incubated at 30 °C and 1000 rpm in a thermomixer. The batch reaction volume was 1 mL. Each specific initial activity measurement consisted of five technical replicates, which were stopped at different distinct points in time (less than 5 min total reaction time) by boiling at 80 °C for 5 min. Next, the reaction solution was tempered to 20 °C for 30 min before taking four technical replicates for chiral HPLC analysis. Only specific initial activities with a correlation of $R^2 \geq 98\%$ in their inclination were considered.

The obtained orthogonal data array of specific initial activities was utilized to determine kinetic reaction parameters by inverse fitting with *fmincon* MATLAB (MathWorks 2017b, USA; parameter constrains see ESI† Table S1).[22] As reaction kinetic formula a Michaelis–Menten kinetic of the 2nd order (eqn (1)) with a substrate inhibition term for acetaldehyde was applied.[15,23] For benzaldehyde no inhibition was detected in the applied concentration range. Hence a benzaldehyde inhibition term is neglected.

$$v = \frac{V_{MAX} \times c_{BA} \times c_{AA}}{(K_{M,BA} + c_{BA}) \times \left(K_{M,AA} + c_{AA} + \frac{c_{AA}^2}{K_{inh,AA}}\right)} \quad (1)$$

Here v [s^{-1}] denotes the reaction velocity, V_{MAX} [s^{-1}] the maximal reaction velocity, c_{BA} [mM] the benzaldehyde concentration, c_{AA} [mM] the acetaldehyde concentration, $K_{M,BA}$ [mM] and $K_{M,AA}$ [mM] denote the Michaelis–Menten coefficients for benzaldehyde and acetaldehyde, and $K_{inh,AA}$ [mM] is the coefficient for reversible acetaldehyde inhibition.[25] A more detailed mechanistic modelling approach of the benzaldehyde lyase reaction under aqueous conditions is discussed by Zavrel *et al.* (2008).[26] Yet, the determination of the many kinetic parameters goes beyond the Ockham's razor approach, which our herein presented work follows.

Cofactor supplementation. Three buffer stock solutions were prepared in which either 5 mM ThDP with 25 mM $MgSO_4$, 2.5 mM ThDP with 12 mM $MgSO_4$, or 0.5 mM ThDP with 5 mM $MgSO_4$ were combined. Each cofactor concentration was investigated by incubating 100 mg mL^{-1} LWCs in either 500 mM benzaldehyde dissolved in MTBE or 240 mM acetaldehyde dissolved in MTBE with 100 μL mL^{-1} of the respective buffer in a batch reaction setup of 0.5 mL (final benzaldehyde concentration in reaction: 250 mM, acetaldehyde concentration: 120 mM). Samples were incubated at 30 °C and 1000 rpm. After 0, 1, 2, 4, 6, 8, and 24 h incubation time the reaction was started by adding the same volume of the respective carboligation substrate (either 500 mM benzaldehyde or 240 mM acetaldehyde stock solutions). The batch reaction volume was 1 mL. Specific initial activities were determined.

Setup of a single continuous stirred tank reactor. The herein described principle for setting up a continuous stirred tank reactor also applies to all below described cSTR-cascade setups. A stirred tank reactor, a polypropylene enzyme membrane reactor (EMR; Forschungszentrum Jülich GmbH, Germany) with a reactor volume of 3 mL as described by Kragl *et al.* was applied (schematic drawing *cf.* ESI† Fig. S1).[24] Notably, the described stir plate was substituted by a magnetic stir bar (30 mm × 6 mm), which led to an increased reactor volume of 9 mL. Upon starting the process, the reaction chamber was flooded with the respective substrate solution in MTBE. In all cases LWCs containing heterologously expressed *Pp*BFD varL461A (formulated as powder, without any preincubation) were placed inside the already flooded chamber and 2 mL of 1 M TEA buffer pH 10 with 5 mM ThDP and 25 mM $MgSO_4$ were added. A PDCF membrane (BioRad, Hercules, USA) with 0.2 μm pores was placed above to retain cells. Any air bubbles were manually pressed out underneath the membrane upon sealing. The reactor was sealed with Krevolast S8 seals (Kremer GmbH, Germany). All cSTR setups were conducted at 30 °C and 300 rpm. In all setup the pumping direction was opposed to gravitation.

Model of a single continuous stirred tank reactor. The enzymatic conversion in a cSTR is mathematically described by mass balances, which account for ingoing and outgoing fluxes, as well as the enzymatic reaction. The model assumes an ideal mixing behaviour of the cSTR with homogeneous spatial concentration and temperature distribution and constant filling volume. The equations for acetaldehyde (AA), benzaldehyde (BA), (*S*)-2-HPP (HPP) and *Pp*BFD varL461A (BFD) concentrations in a reactor with one feed and one outlet (schematically shown in Fig. 2B) are given in eqn (2a)–(c).

$$\frac{dc_{i,BA}}{dt} = \frac{F_i}{V}c_{i,BA}^{in} - \frac{F_i}{V}c_{i,BA} - c_{i,BFD}v \quad (2a)$$

$$\frac{dc_{i,AA}}{dt} = \frac{F_i}{V}c_{i,AA}^{in} - \frac{F_i}{V}c_{i,AA} - c_{i,BFD}v - c_{i,AA}v_D \quad (2b)$$

$$\frac{dc_{i,HPP}}{dt} = -\frac{F_i}{V}c_{i,HPP} + c_{i,BFD}v \quad (2c)$$

F_i [m^3 s^{-1}] describes the volumetric flow rate of reactor unit $i \in \{1, 2, 3\}$, while $c_{i,XX}$ [mM] is the concentration of compound XX (benzaldehyde (BA), acetaldehyde (AA), or (*S*)-2-HPP (HPP)) in the reactor. The enzyme concentration is denoted by $c_{i,BFD}$ and accounts for irreversible enzyme deactivation (see ESI† S9 for details). The enzymatic reaction velocity v [s^{-1}] as defined in eqn (1), accounts for reversible enzyme inhibition, the velocity v_D accounts for the loss of acetaldehyde that is bound to the deactivated enzyme, which could be neglected but is considered for completeness of the mass balance, and V [m^3] is the reactor volume.

Optimal biocatalyst load. 20 mg mL^{-1}, 100 mg mL^{-1} and 200 mg mL^{-1} of LWCs were tested in a reaction setup of only one cSTR (setup schema ESI† Fig. S2A). The substrate solution contained a concentration $c_{1,BA}^{in}$ of 250 mM benzaldehyde and $c_{1,AA}^{in}$ of 100 mM acetaldehyde dissolved in MTBE and pumped (HPLC pump, ThalesNano, US) at F_1 = 0.3 mL min^{-1}. Samples were manually collected at the cSTR outlet at distinct points in time. Sample preparation and analysis are described below.

Acetaldehyde dependent long-term deactivation. To investigate the impact of acetaldehyde dependent deactivation on *Pp*BFD varL461A over time, a reaction setup with only the first cSTR unit (setup schema ESI† Fig. S2A) was applied. The feed concentration $c_{1,BA}^{in}$ was set to 250 mM benzaldehyde with a variable acetaldehyde amount $c_{1,AA}^{in}$ of either 60 mM, 80 mm, 100 mM, 120 mM, 150 mM, or 250 mM in MTBE. Pumping velocity F_1 was set to 0.3 mL min^{-1}, except for $c_{1,AA}^{in}$ 150 mM and 250 mM, pumped at a flow rate of 0.1 mL min^{-1} to warrant steady-state conditions inside the reactor. 100 mg mL^{-1} *Pp*BFD varL461A LWC were applied. Samples were manually collected at the cSTR outlet at distinct points in time. Sample preparation and analysis are described below.

Modelling acetaldehyde dependent long-term deactivation. An irreversible deactivation kinetic for *Pp*BFD varL461A was set up. This deactivation model considers that *Pp*BFD varL461A is a tetramer. The four active sides are located between the conjunctions of respective monomers.[27] The irreversible deactivation is described by a step-wise denaturation of the respective monomers in 16 different states of deactivation (see ESI† chapter S9 for a more detailed description).[15,28] Within this manuscript, it is referred to as staged deactivation model. As the tetramer is ordered like a dimer of dimers, the activity of each monomer most likely contributes to the activity of two active sites. The concrete nature of the deactivation-mechanism is currently not known. The velocity of the deactivation process of each monomer is hypothesized to depend linearly on the acetaldehyde concentration. The probability of each monomer to be denatured by acetaldehyde is assumed to be equal and thus expressed by the same deactivation coefficient k_D. Consequently, the concentration of active enzyme c_{BFD} [mmol g^{-1}_{LWC}] is modelled as the sum of the concentrations of three isoenzyme groups. Alternatively, a simple generic approach for modelling enzyme deactivation is tested for comparison. In this model, the enzyme is completely deactivated in one step.

The resulting differential equation system was solved using the ode15s solver in MATLAB 2017b. For initial conditions inside the reactor, the corresponding inlet concentrations $c_{i,XX}^{in}$ were used. Since LWC instead of purified enzymes are used, the amount of *Pp*BFD varL461 is estimated by assuming that one dry *E. coli* cell weighs 280 fg, of which 155 fg accounts for the total protein.[29,30] Of this total protein content 58% are assumed to be *Pp*BFD varL461. This accounts for a total *Pp*BFD varL461 concentration of 15.8 mmol g^{-1}_{LWC} based on a molecular enzyme weight of 57 kDa.[31,33]

Determination of optimal acetaldehyde stock solution concentration and flow into the cSTR-cascade units 2 and 3. In the cSTR-cascade setup acetaldehyde is added to unit 2 and 3 at the respective inlets. Therefore, an acetaldehyde stock solution with c_2^{stock} = 3.5 M was prepared to determine the optimal flow rates for this stock solution (F_2^{stock}). For prolonged process stability with high benzaldehyde conversion, a simplified technical setup was used. The setup consisted of a single cSTR-cascade unit, with flux F_2, whose influx is composed of two streams, F_1 and F_2^{stock}, that are combined in a T-mixing unit (setup schema ESI† Fig. S2B). The substrate solution of the first stream contained $c_{1,BA}^{in}$ 170 mM, $c_{1,AA}^{in}$ 10 mM and $c_{1,HPP}^{in}$ 90 mM and was pumped at F_1 300 μL min^{-1} by a HPLC pump (ThalesNano, US). The stock flow rate F_2^{stock} was varied between 8 and 12 μL min^{-1} (Asia Syringe Pump, Syrris, Royston, UK) with an acetaldehyde concentration of 3.5 M. Samples were collected manually at the cSTR outlet. Sample preparation and analysis are described below.

Synthesis of (*S*)-2-HPP in a stirred tank reactor cascade. Three cSTR units were aligned in series to a cSTR-cascade (setup schema ESI† Fig. S2C). The substrate solution contained $c_{1,BA}^{in}$ 250 mM and $c_{1,AA}^{in}$ 100 mM in MTBE. The respective

acetaldehyde stock solutions c_2^{stock} and c_3^{stock} contained 3.5 M acetaldehyde dissolved in MTBE. Pumping velocities in the setup were adjusted accordingly to F_1 300 μL min^{-1}, F_2^{stock} 9 μL min^{-1}, and F_3^{stock} 8 μL min^{-1}. Samples were collected manually at the outlet of the third cSTR. Sample preparation and analysis are described below.

Modelling of a continuous stirred tank reactor cascade with 3 units. A model describing the cSTR-cascade in Fig. 2B was established by connecting the outlet of the first unit with the inlet of the second and the outlet of the second unit with the inlet of the third. The flow rates of the second and third units are increased by the feed rates from the added stock solutions according to eqn (3a) and (b).

$$F_{i+1} = F_i + F_{i+1}^{stock} \quad i \in \{1, 2\} \tag{3a}$$

$$\frac{c_{i+1,in}}{F_{i+1}} = \frac{c_i^{out}}{F_i} + \frac{c_{i+1}^{stock}}{F_{i+1}^{stock}} \quad i \in \{1,\ 2\} \tag{3b}$$

F_{i+2}^{stock} is defined as the volumetric flow rate [m^3 s^{-1}] of the acetaldehyde stock solution (Fig. 2B) entering the respective reactor unit number $i \in \{2, 3\}$. The resulting differential equation system for describing the cSTR cascade was also solved using the ode15s solver in MATLAB 2017b.

Product isolation. The collected product solution was dried with $MgSO_4$ and filtered through a glass frit. The dried solution was concentrated under reduced pressure on a Rotavapor (Büchi, Essen, Germany) reducing MTBE. The concentrated solution was overlaid with 20% (v v^{-1}) pure petrol ether and stored for 16 h at 4 °C. Formed crystals were separated by filtration through a Schleicher & Schuell 589^2 filter (white ribbon, Schleicher & Schuell, Germany). Obtained crystals were washed with 4 °C cooled petrol ether and dried at room temperature. For purity analysis, crystals were solubilized in 70% *n*-heptane/30% 2-propanol and analysed as described below.

Substrate screening for *Pp*BFD varL461A. Benzaldehyde and derivatives thereof were screened for conversion with *Pp*BFD varL461A. 40 mM benzaldehyde (or derivative) and 120 mM acetaldehyde were dissolved in MTBE and added to 20 mg mL^{-1} *Pp*BFD varL461A LWCs in 1 mL batch setups. Reactions were started by the addition of 20 μL mL^{-1} 1 M TEA buffer pH 10 containing 5 mM ThDP and 25 mM $MgSO_4$. Reactions were incubated at 1000 rpm and 30 °C for 24 h. Experiments were performed in triplicates. Sample preparation and analysis as described below.

For continuous synthesis of *p*-methoxy benzaldehyde, three cSTR units were aligned in series as depicted in Fig. 2B. The concentration $c_{i,XX}^{in}$ contained 250 mM *p*-methoxy benzaldehyde and 100 mM acetaldehyde in MTBE. The respective acetaldehyde stock solutions c_2^{stock} and c_3^{stock} contained 3.5 M acetaldehyde dissolved in MTBE. Pumping velocities in the setup were adjusted accordingly to F_1 100 μL min^{-1}, F_2^{stock} 4 μL min^{-1}, and F_3^{stock} 3 μL min^{-1}. Samples were collected manually at the outlet of the third cSTR unit. Sample preparation and analysis are described below.

Analytics

HPLC analytics. Chiral HPLC analysis was conducted on a Dionex 3000 UHPLC System (Thermo Fisher Scientific, Waltham, USA). Samples were separated on a ChiralPak IA (Daicel, Germany) column (250 × 4.6 mm; 5 μm) at isocratic conditions of 70% *n*-heptane/30% 2-propanol at a flow of 1.5 mL min^{-1}. The sample tray was tempered to 20 °C and the column oven to 25 °C. Toluene was applied as internal standard. Samples eluted in the following order: toluene (210 nm) 2.18 min, benzaldehyde (244 nm) 2.72 min, and (*S*)-2-hydroxy-phenylpropanone (244 nm) 3.33 min, (*R*)-2-hydroxy-phenylpropanone (244 nm) 3.79 min. Derivates eluted in the same order with a minor time shift (exact times listed in ESI† Table S2).

NMR analytics. ^{1}H NMR spectra were recorded on a Bruker Advance DRX 600 MHz (Bruker, Billerica, USA). Obtained spectra were in accordance with literature (see ESI,† Fig. S10 and S11).[6,8]

Results and discussion

Optimal substrate concentrations in a MARS (batch determination)

First the optimal paring of substrate concentrations in MARS was investigated in batch experiments. With regard to high reaction rates an initial activity screening was performed with acetaldehyde ranges from 25 mM to 200 mM paired with benzaldehyde concentrations from 50 mM to 300 mM.

The screening revealed an acetaldehyde optimum between 60 to 100 mM in terms of initial activity, determined within up to 5 min reaction time (Fig. 3). Higher concentrations resulted in an activity decline, which is assumed to be due to substrate inhibition. These findings are consistent with batch

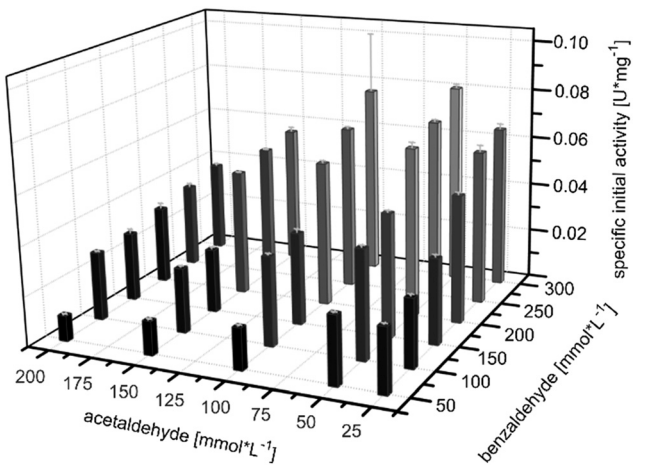

Fig. 3 Initial activity measurements. The initial catalytic velocity of *Pp*BFD varL461A for (*S*)-HPP synthesis at substrate concentrations of 25 to 200 mM acetaldehyde and 50 to 300 mM benzaldehyde was measured; 30 °C, 1000 rpm, $n_{technical}$ = 4.

observations for *Pp*BFD varL461A in MARS by others.[17] Compared to *Pp*BFD reactions in buffer environment with an acetaldehyde optimum at 400 mM to 500 mM, the reaction in MARS presented here shows its acetaldehyde optimum at four times lower concentrations.[9,12,13] At first glance, this finding was unexpected. A possible explanation can be the polar nature of acetaldehyde, which would favour an inhomogeneous distribution in MARS, meaning it locally accumulates in the hydrate shell of the biocatalyst. Therefore, the local concentrations of acetaldehyde could hypothetically be higher and correspond more to the optimum in the buffer.

In case of benzaldehyde, the initial activities obtained a local high at 300 mM (Fig. 3). To identify, whether this local benzaldehyde optimum also corresponded to a global maximum, the screening was extended to benzaldehyde concentrations of up to 5 M (ESI† Fig. S3). Since no synergistic effects were observed between the ratio of acetaldehyde and benzaldehyde, this extended screening was performed with only one acetaldehyde concentration of 100 mM. The extended screening showed that in fact concentrations of up to 500 mM lead to an increased initial activity before it declines again (ESI† Fig. S3). Hence, MARS can be a suitable reaction environment for high aromatic substrate concentrations, which can circumvent long term enzyme deactivation due to substrate toxicity.

Calculation of apparent kinetic parameters and substrate inhibition in a MARS (batch determination)

Next, kinetic parameters for the carboligation towards (*S*)-2-HPP by *Pp*BFD varL461A in a lyophilised whole cell formulation in MARS were obtained by fitting the initial activity screening results (Fig. 3) with the 2nd order Michaelis–Menten (eqn (1)). This results in a reaction-kinetic model, which is designed to be later coupled to the mechanistic cSTR-c model. It is possible that the substrate and product concentrations within the lyophilized whole cells (LWCs) and the liquid phase are different. As the concentrations in the cells cannot be detected, an even distribution was assumed for the calculations. Consequently, only apparent parameters could be calculated.

This first fit resulted in a V_{MAX} of 9.2 U mg^{-1} for LWC catalyst formulations, a $K_{M,BA}$ of 278.3 mmol L^{-1}, a $K_{M,AA}$ of 1693.4 mmol L^{-1}, and an inhibitory constant $K_{inh,AA}$ of 1.8 mmol L^{-1}. When evaluating these results, it has to be stressed that they are numerical results obtained with a Mathlab solver within defined limits (Table S1†). While the values themselves may not reflect real values, otherwise a reaction would hardly take place, they are the best obtained fit based on the orthogonal initial activity matrix and model within the defined limits. Probably, other presently unknown variables of the non-natural reaction environment besides acetaldehyde have an influence on the catalyst performance.

For a subsequent cSTR-c application, a setup of three cSTR-c units in series were investigated. Based on the restriction to three cSTR-c units it was estimated that 250 mM benzaldehyde can be converted with acetaldehyde amounts being added slightly above the equimolar amount.

Transfer of operation parameter into one cSTR-cascade unit (continuous)

I. Optimal catalyst concentration. The findings were first applied to one cSTR unit with the aim to define the optimal catalyst load. In a cSTR unit the biocatalyst retainment is realized by a membrane holdback. In the initial activity screening in a batch reaction setup, 20 mg L^{-1} LWC had been applied. In a transfer to continuous operation biocatalyst loads between 20 mg L^{-1} to 200 mg L^{-1} were tested. As expected, higher catalyst loads resulted in increased activity, though biocatalyst loads above 100 mg L^{-1} resulted in membrane blockage over time. To counter this effect, different stirrer bars and stirrer speeds, various membrane types with different repelling surfaces and pumping against gravity were investigated (data not shown). Since all these activities did not significantly improve the problem, 100 mg L^{-1} was evaluated as a route for further setups. In plug flow reactors increased biocatalyst loadings are associated with extended enzyme half-life.[32] An increase in LWC quantities in our setup did not lead to significantly prolonged stability. This can be due to the difference in the substrate concentration profile between a cSTR unit and a plug flow reactor. The essential difference between these two is, that in a plug flow reactor substrate concentrations decrease over the length of the column, whereas in a cSTR-c unit the amount of substrate is ubiquitously distributed under optimal conditions. Thus, in a plug flow reactor biocatalyst at the beginning of the column exhibits a faster deactivation rate than at the end of the column, while in a cSTR-c unit the deactivation rate of all catalysts is the same for all LWCs. This also reveals a limitation of a cSTR-c process in the emulation of a counter flow reactor, when it is extended to a cross flow reactor setup (Fig. 2A and B).

II. Optimal cofactor concentration to achieve high biocatalyst stability. In a next step, the half-life of the biocatalyst in one cSTR-c unit was subject of optimisation. In literature, the supplementation of the two cofactors ThDP and Mg^{2+} is reported to have a stabilizing effect on the isolated *Pp*BFD varL461A in buffered reactions. ThDP is directly involved in the catalytic cycle of *Pp*BFD varL461A and Mg^{2+} anchors ThDP in the active side of the biocatalyst.[8,11,33,34] Whether a similar stabilizing effect would be observed in MARS was investigated by supplementing up to 1.1 mM ThDP and 5.5 mM Mg^{2+} in the reaction setup, which was added in the preparation to the buffer fraction.‡ Notably, the lyophilization process of the whole cell catalyst during LWCs formulation causes membrane perforation,

‡ Concentrations in the buffered stock solution were up to 5 mM ThDP and 25 mM $MgSO_4$.

which is assumed to facilitate diffusion into the cell by a great extent.[21,35] The results of this supplementation experiment revealed the highest applied cofactor concentration as most beneficial to warrant a stable catalytic activity for 8 h before a deactivation of approximately 60% sets in (data not shown). In the negative control without supplements a deactivation of 80% was observed already after 4 h (data not shown). These findings indicated endogenous ThDP concentrations as insufficient when production levels of heterologously expressed *Pp*BFD varL461A in the LWCs are very high. This conclusion would be contrary to literature, which reports abundant endogenous cofactor supply as an intrinsic benefit of whole cell catalysts.[21] To evaluate the validity of this conclusion a rough estimate of intracellular ThDP concentrations was performed based on literature values of endogenous metabolite concentrations.[36] According to this estimation, there is a demand of 8000 fold more ThDP than LWCs would intrinsically provide (estimation *cf.* ESI† S7). A detailed analysis of real endogenous metabolite concentrations could be gained by instrumental analytics like MS-based metabolism methods.[37,38] Hence, 5 mM ThDP and 25 mM Mg^{2+} were supplemented to the buffer, which was then added to the MARS system directly in the cSTR chamber. Notably, the possibility of cofactor leakage from the hydrophilic cell interior into the organic system was estimated to be low, as both cofactors are highly polar and are believed not to dissolve in the MTBE based substrate solution in high amounts.

Determination of acetaldehyde dependent deactivation

During kinetic parameter investigation, the influence of different acetaldehyde concentrations on initial rate activity was determined. Now, the acetaldehyde dependent deactivation term k_D of *Pp*BFD varL461A was examined. Therefore, acetaldehyde concentrations in a range of 60 mM to 250 mM were investigated over time in one cSTR unit (technical setup scheme *cf.* ESI† Fig. S2A). The determination of k_D is essential to find optimal acetaldehyde concentrations and therewith an acetaldehyde feed for the three cSTR-c units. The experimental results verified a proportional correlation of acetaldehyde concentration and enzyme deactivation (Fig. 4). Enzyme deactivation is here derived from a decline in (*S*)-2-HPP formation.

The process model (eqn (3a) and (b)) was fitted to the experimentally retrieved data to determine the enzyme deactivation term k_D to quantitatively describe the long-term process. The obtained model was able to describe measured benzaldehyde conversions in a single cSTR unit in combination with acetaldehyde concentrations of up to 120 mM very well (ESI† Fig. S5C). For higher acetaldehyde concentrations, the long-term conversion profile deviated considerably from measured data. Hence, the Michaelis–Menten parameters were re-estimated together with k_D using a genetic algorithm and gradient search in MATLAB (ESI† Fig. S5). The re-estimation revealed that Michaelis–Menten kinetic parameters under process conditions in a single cSTR unit have a marginally (by 0.1 U mg^{-1}) different V_{MAX} of 9.3 U mg^{-1}, but a 5-fold increased $K_{inh,AA}$ of 9.9 mM, while K_M values for acetaldehyde and benzaldehyde remained unaffected. The re-estimated k_D was 2.1×10^{-6} s^{-1}. These process Michaelis–Menten parameters were found to describe the conversion of benzaldehyde to (*S*)-2-HPP in one cSTR-cascade unit more adequately than the previously determined parameters from initial activity measurements (Fig. 4). The kinetic differences are likely caused by altered mass transfer in the 9 mL cSTR-c unit with internal stirring as compared to the 1 mL batch experiments with external stirring in which the initial activities were recorded. Importantly, the process

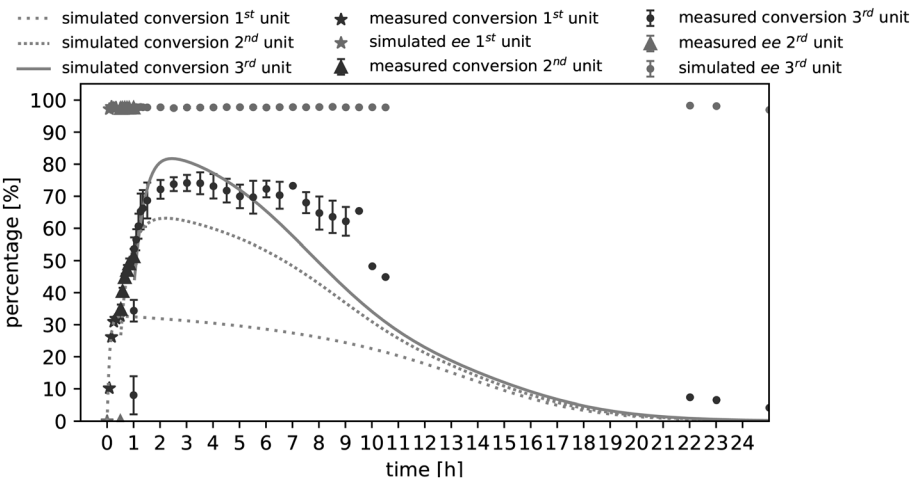

Fig. 4 Continuous operation of a cSTR-cascade consisting of 3 units. The staged deactivation model was used, and the Michaelis–Menten parameters were estimated from process data of a single cSTR unit. Displayed is the conversion over the whole cSTR-cascade. At the beginning, the first cSTR unit is filled (star) and then eflux flows into the second unit (triangle) and then in the third (dots). A measurement in the 1st and 2nd unit is omitted by the technical setup once they are connected to the subsequent unit, as measurement is conducted at the efflux position. Here, the simulated data projects the conversion over time in the respective units.

kinetic parameters together with k_D described an ideal acetaldehyde concentration of 100 mM. This finding aligns with the experimental data gained in initial activity screenings in batch. Conclusively, 100 mM acetaldehyde was applied in further setups as this concentration yields the best compromise between fast catalytic velocity due to sufficiently high amounts of acetaldehyde, low acetaldehyde initial rate inhibition, and a relatively low enzyme deactivation rate over time (ESI† Fig. S5).

Acetaldehyde addition in a two-unit setup to identify optimal feeds for a continuous stirred tank reactor cascade. The next objective was to conjunct three cSTR units to obtain a cSTR-cascade with the challenge of equal acetaldehyde distribution across these three units (Fig. 2B). To achieve this aim, optimal acetaldehyde feeds for unit two and three had to be tested first. Therefore, highly concentrated acetaldehyde stock§ was added to unit two and three. Different flow rates of a 3.5 M stock solution were investigated with focus on maximum (*S*)-2-HPP conversion without readjusting the retention. This was realized by providing one cSTR-cascade unit with two feeds (setup scheme *cf.* ESI† Fig. S2B). One feed F_1, with flowrate of 300 μL min^{-1}, represents the efflux of a prior first cSTR unit with fixed concentrations of 170 mM benzaldehyde, 10 mM acetaldehyde, and 80 mM. The second feed was a 3.5 M acetaldehyde solution, whose velocity F_2^{stock} was varied from 8 to 12 μL min^{-1} to control the amount of continuously provided acetaldehyde. A flow rate of 9 μL min^{-1} exhibited the best result for the second unit (ESI† Fig. S6). This yields a total conversion of 64% (160 mM (*S*)-2-HPP) in the outflux of the second unit (*cf.* ESI† Fig. S6). As the conversion from the first unit was 36% (with respect to the fed 250 mM benzaldehyde), conclusively a conversion increase by 28% to the prior unit was detected. Notably, 8 μL min^{-1} also yielded reliable results, which is worthy to consider for the third CSTR-cascade unit. As pointed out above, acetaldehyde accumulates over the cSTR-cascade. Thus, the third unit could benefit from this reduced flow rate of 8 μL min^{-1} acetaldehyde stock.

Operation of a three-unit cSTR-cascade. The determined parameters for optimal starting concentrations $c_{1,AA,in}$ for acetaldehyde (100 mM) and $c_{1,BA,in}$ for benzaldehyde (250 mM) as well as flow velocities F_2^{stock} (9 μL min^{-1}) and F_3^{stock} (8 μL min^{-1}) for a 3.5 M acetaldehyde stock solution were applied to convert 250 mM benzaldehyde continuously in a cSTR-c (Fig. 2B). With this experimental setup, over 8 h a stable output of 190 mM (*S*)-2-HPP (76% conversion; Fig. 4) with an ee of 98% could be achieved. It is noteworthy that the 76% conversion is close to the thermodynamic equilibrium for this reaction under buffered conditions, which corresponds to a 78% conversion of benzaldehyde.[8] The first unit had an output of 93.5 mM (*S*)-2-HPP, which increased in the second unit to 155 mM (*S*)-2-HPP followed by 190 mM final concentration after unit 3.

Comparison of simulation and conversion determination of a three-unit cSTR-cascade. The mechanistic model with a single deactivation stage and parameters estimated from process data of a single cSTR unit predicted a slightly higher maximum conversion for a cSTR-cascade with three units when compared to empiric measurements (Fig. 4). It correctly described the infliction point of conversion over time, but overestimated the rate of conversion decline. In the experiment, a slight conversion decrease sets in after about 2.5 h and after 16 h the catalyst is almost completely deactivated (Fig. 4). The deviation between model and measured data could be caused by an unknown deactivation mechanism or an unknown concentration distribution between the reaction environment and LWCs. The influence of the deactivation mechanism was evaluated by comparing the staged deactivation model with 16 deactivation states and a simple generic model with only one deactivation stage. The results of these models differed less than the variance of the respective measurements (data not shown). Hence, equally accurate predictions can be made with either mode. The exact nature of the deactivation mechanism cannot be elucidated with the available data and would required further experimental investigation and complex analytics. The deviation between model and measured data is further amplified by a potentiation of enzyme deactivation along the cSTR-cascade, *i.e.* as the catalyst in the first unit is deactivated, more acetaldehyde reaches the second unit, which further accelerates deactivation, and so on. The conversion profile over time is much better reproduced by the model when the acetaldehyde concentration in the inflow of each reactor is reduced to 60% of the respective original value (see ESI† Fig. S5), at a slightly reduced absolute conversion rate. This indicates that amounts of acetaldehyde in the reactors, which could not be measured with the analytical tools in hand, could indeed be lower than considered by the model. In the future, potentially new methods for real-time online quantification of acetaldehyde may enable an integrated model based process control. Thus, a feedback loop controls the acetaldehyde pump velocity based on measured acetaldehyde concentration and the model. The integration of such a loop may further optimize the final conversion achieved with the cSTR-cascade.

Advantages of cSTR-cascade system compared to a fed-batch reaction mode. The herein established cSTR-cascade can be compared to in literature reported (*S*)-2-HPP synthesis in MARS under fed-batch conditions. This fed-batch allowed an even higher product titre of 360 mM (*S*)-2-HPP in MARS[17] compared to the 190 mM (*S*)-2-HPP gained in the cSTR-cascade. Though these concentrations appear tempting to prefer a discontinuous synthesis, the overall productivity of both processes and their respective specific space–time-yields (sSTY) are important criteria as well. Both parameters reflect the synthesis efficiency in

§ Notably, the low density of acetaldehyde made it technically impossible to pump pure acetaldehyde and required a concentration below 4 M in MTBE to obtain reliable pumping.

Table 1 Fed-batch process values against the herein presented continuous process. Presented fed-batch values were obtained in a micro-aqueous reaction system by Wachtmeister *et al.* 2014.[17] LWC = lyophilized whole cells

Process operation	Catalyst	Conversion [%]	Final (*S*)-HPP concentration [M]	ee [%]	Retention time [h]	Catalyst load [g L^{-1}]	sSTY [g L^{-1} d^{-1} $g^{-1}_{catalyst}$]
cSTR-c	LWC	76	0.19	98	0.5	100	0.190
Fed-batch	LWC	68	0.34	98	6	100	0.085

relation to the biocatalyst used, which is a significant cost driving factor in biocatalytic reaction arrangements.[39,40] The continuous setup used in this manuscript exhibits higher sSTY of 0.190 g L^{-1} h^{-1} $g^{-1}_{catalyst}$ compared to the fed-batch approach with 0.085 g L^{-1} h^{-1} $g^{-1}_{catalyst}$ (Table 1). In terms of productivity, the continuous process with 4.56 g g^{-1}_{LWC} even exceeds the fed batch configuration by a factor of 9, due to the intrinsic enzyme recycling in the cSTR, which allows the catalyst to be used over several retention times. The comparison of the herein established cSTR-cascade reduces catalyst costs for the synthesis of (*S*)-2-HPP by a remarkable factor of 180 compared to the fed-batch process (*cf.* ESI† S8). Still, the costs of biocatalyst production are by a factor of two too high for an acceptable economic return. But this is only a rough estimation according to average values by Tufvesson *et al.*[41] and not case specific for our product. In general, the results proof the advantage of a continuous process operation mode and inherent catalyst recycling with respect to process operation costs. In addition, the setup emphasizes the potential of the continuous MARS synthesis. When coupled with improvements in catalyst stabilization, *e.g.*, through protein engineering or other stabilizing measures like additives, even better values would be achievable.

Product isolation

In a next step, the synthesized (*S*)-2-HPP was purified with the aim to gain an *in situ* product crystallization. Thus, the physicochemical parameters of all compounds were collected to deduce a suitable downstream process (ESI† chapter V, Table S3). In a step-wise distillation at mild vacuum both, acetaldehyde and MTBE, were successfully stripped from the product solution (Fig. 5). The remaining product mixture contained benzaldehyde and (*S*)-2-HPP. Unfortunately, benzaldehyde could not be stripped from the solution at 50 °C and full vacuum. Following the ideal gas law, the temperature could in theory be increased to strip benzaldehyde. This strategy was not followed, as a temperature increase might reduce the stereoselectivity and regioselectivity of the product, as (*S*)-2-HPP is prone to tautomerise at higher temperatures. Hence, a separation based on the distinguished melting points of both chemicals was performed by cooling crystallisation at 4 °C. Under these conditions (*S*)-2-HPP crystals grew within a few hours. Upon filtration and washing with cooled petrol ether, an isolated yield of 68% with a crystal purity of 99% was achieved. This simple technique, moderate vacuum combined with a cooling crystallization, underscores the advantages of MARS in terms of product isolation. In addition, other products are reported to have been isolated from MARS by crystallization.[6] Combined, the presented results demonstrate that MARS is an easily applicable reaction system enabling facile product isolation by crystallization.

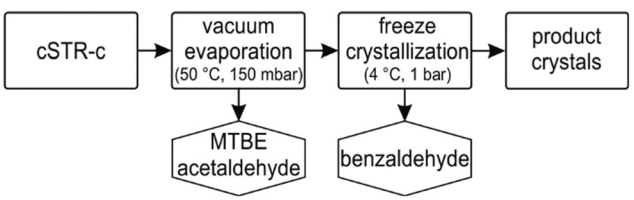

Fig. 5 Block flow diagram for (*S*)-HPP isolation.

Substrate range screening to broaden product platform

Having established a robust synthesis process for (*S*)-2-HPP with an easy and fast product isolation, it would be desirable to use the process to gain access to a whole (*S*)-2-HPP derivative platform, which can be used for further chemical syntheses. Hence, nitro-, halo-, and methoxy-derivatives of benzaldehyde substituted at the *ortho*-, *meta*-, and *para*-position were screened for mixed carboligation products with acetaldehyde with the enzyme *Pp*BFD varL461A. The outcome of this substrate range screening in MARS revealed, that all (*S*)-2-HPP derivatives except for the *meta*-nitro derivative can be produced (Table 2). Even more convincing is the exceptional ee of >99%, which was obtained for almost all derivatives when using *Pp*BFD varL461A. Also, chemoselectivity was excellent, as no phenylacetylcarbinol (IUPAC: 1-hydroxy-1-phenyl-propan-2-one) derivatives were detected.

Transfer of cSTR-c to an a *para*-methoxylated (*S*)-2-HPP derivative

As an example, *para*-methoxy-benzaldehyde was selected to proof transferability of the cSTR-c to (*S*)-2-HPP synthesis to other products. In a quick proof-of-principle without determination of kinetic parameters, already 41% conversion with an ee of 99% could be obtained (ESI† Fig. S9, for ^{1}H-NMR determination see S11) without any product specific optimization. This is almost equally as good as a recently presented fed-batch process optimized in MARS, which achieved a 46% conversion of *para*-methoxy benzaldehyde to the target (*S*)-2-HPP derivative.[6] A determination of kinetic

Table 2 Conversion of benzaldehyde-derivatives (40 mM) in a reaction with a three-fold excess of acetaldehyde (120 mM) and lyophilised wet cells containing *Pp*BFD varL461A in micro-aqueous reaction system to form the respective substituted (*S*)-HPP product

	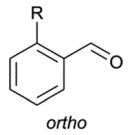 *ortho*		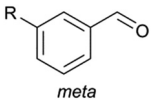 *meta*		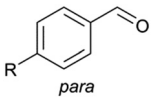 *para*	
	Conv. [%]	ee [%]	Conv. [%]	ee [%]	Conv. [%]	ee [%]
R = F	82	84	95	99	58	99
R = Cl	22	99	87	96	48	99
R = Br	8	99	81	99	45	99
R = MeO	19	99	85	96	56	95
R = NO_2	33	99	1	69	99	99

parameters would certainly help to further improve reaction conditions in the cSTR and thus lift it to levels of the fed-batch process or even beyond. But this resource- and time-saving rapid transferability test already shows that the presented cSTR-cascade is a stable synthesis system that can even be transferred to other substrates to obtain a product platform of (*S*)-2-HPP derivatives.

Summary and conclusion

The herein presented work combines the strengths of a MARS environment, continuous process operation, and model-driven process optimization to selectively obtain 190 mM (*S*)-2-HPP with an ee > 98% over 8 h.

First, kinetic behaviour of applied *Pp*BFD varL461A LWCs in MARS was analysed to determine ideal starting concentrations of the carboligation substrates benzaldehyde and acetaldehyde. It was shown that benzaldehyde concentrations of up to 500 mM and acetaldehyde up to 100 mM can be applied before substrate inhibition sets in. The collected data was used subsequently to deduce apparent Michaelis–Menten parameters. Based on the kinetic data, a continuous process in a cSTR-cascade was selected to minimize effects of substrate inhibition and enzyme deactivation (Fig. 2). Second, options for enhancing catalyst stability were explored to prolong continuous operation. This revealed the supplementation of 5 mM ThDP with 25 mM Mg^{2+} in the 22% (v v^{-1}) MARS buffer fraction as beneficial for enhanced stability. Moreover, the distribution of acetaldehyde over the cSTR-cascade was found to be vital, as enzyme deactivation was observed to be caused by elevated acetaldehyde concentrations. For quantifying this, a novel enzyme deactivation kinetic was proposed that describes the deactivation of the tetrameric *Pp*BFD varL461A as combination of the independent deactivation of its monomers. The final reaction model determined concentrations of 120 mM acetaldehyde as threshold level, beyond which enzyme deactivation accelerates disproportionately fast. This was accounted for by distributing the total acetaldehyde amount which is required to convert 250 mM benzaldehyde over three cSTR-units. The model was also used for computing acetaldehyde stock solution flow rates $F_{i,\mathrm{stock}}$ (Fig. 2B) that prevent an exceeding of 100 mM acetaldehyde in the respective cSTR-cascade units. Third, all determined process parameters were successfully applied for design a cSTR-cascade with a productivity of 4.56 g g^{-1}_{LWC} (*S*)-2-HPP. The whole synthesis process was supported by a mechanistic model with staged deactivation, which illustrated the kinetic reaction behaviour in this continuous reaction setup in an unconventional reaction environment. Although the continuous (*S*)-2-HPP synthesis established here delivers lower product titres compared to an established fed-batch process, a doubled sSTY could be achieved due to catalyst retention and reuse. Hence, the economic feasibility of biocatalytic processes is significantly increased by continuous process operation. In a subsequent downstream processing the organic reaction environment MARS facilitated product isolation and permitted direct product crystallization with an isolated yield of 68% and a crystal purity of 99%. Ultimately, a substrate screening with *Pp*BFD varL461A was performed to identify 2-hydroxy ketone derivatives which are also accessible *via* this process setup. Among all tested bromo-, chloro-, fluoro-, methoxy-, and nitro-derivatives at the *ortho*, *meta*, and *para* position, only *meta*-nitro-benzaldehyde could not be converted. All others exhibited excellent enantio- and regioselectivity. Among them *para*-methoxy-benzaldehyde was transferred in a proof of principle into the setup cascade and yielded in an unoptimized state already 41%. This verifies the potential of this technical setup in combination with the enzyme to be applicable for the production of a product platform.

Conclusively, this biocatalytic reaction system appeals with its continuous output of high product concentrations and an microaqueous reaction environment granted by MARS. This quite possibly could facilitate a vast implementation of biocatalysis in complex continuous flow synthesis (*e.g.* unconventional reaction environment) in the near future.

Abbreviations

c	Concentration [mM]
cSTR	Continuous stirred tank reactor

cSTR-c	Continuous stirred tank reactor cascade
F	Flow velocity [m^3 s^{-1}]
2-HPP	2-Hydroxy-1-phenylpropanone
LWC	Lyophilized whole cells
MARS	Micro-aqueous reaction system
$MgSO_4$	Magnesium sulfate
*Pp*BFD	*Pseudomonas putida* benzoylformate decarboxylase
MTBE	Methyl *tert*-butyl ether
τ	Retention time
TEA	Triethylamine
ThDP	Thiamine diphosphate
V	Reactor volume [m^3]

Conflicts of interest

There are no conflicts to declare.

Acknowledgements

We would like to acknowledge the Helmholtz-Association within the framework of the young investigator's group "synthetic enzyme cascades" for funding this project. Further we thank the company Alfa Laval for their valuable input on membrane selection. Also, we thank Christoph Westerwalbesloh and Martina Pohl for fruitful discussions on kinetics and process modelling. Many thanks go to Lilia Arnold for her great investment in the practical work of this academic piece.

Notes and references

1 S. G. Newman and K. F. Jensen, *Green Chem.*, 2013, **15**, 1456–1472.
2 I. R. Baxendale, L. Brocken and C. J. Mallia, *Green Process. Synth.*, 2013, **2**, 211–230.
3 U. T. Bornscheuer, *Philos. Trans. R. Soc., A*, 2018, **376**, 1–5.
4 R. León, P. Fernandes, H. M. Pinheiro and J. M. S. Cabral, *Enzyme Microb. Technol.*, 1998, **23**, 483–500.
5 H. Meyer, E. Eichhorn, S. Hanlon, S. Lütz, M. Schürmann, R. Wohlgemuth and R. Coppolecchia, *Catal. Sci. Technol.*, 2013, **3**, 29–40.
6 R. Oeggl, T. Maßmann, A. Jupke and D. Rother, *ACS Sustainable Chem. Eng.*, 2018, **6**, 11819–11826.
7 A. Jakoblinnert and D. Rother, *Green Chem.*, 2014, **16**, 3472–3482.
8 D. Gocke, L. Walter, E. Gauchenova, G. Kolter, M. Knoll, C. L. Berthold, G. Schneider, J. Pleiss, M. Müller and M. Pohl, *ChemBioChem*, 2008, **9**, 406–412.
9 W. H. De Camp, *J. Pharm. Biomed. Anal.*, 1993, **11**, 1167–1172.
10 T. Dünnwald, A. S. Demir, P. Siegert, M. Pohl and M. Müller, *Eur. J. Org. Chem.*, 2000, **2000**, 2161–2170.
11 H. Iding, T. Dünnwald, L. Greiner, A. Liese, M. Müller, P. Siegert, J. Grötzinger, A. S. Demir and M. Pohl, *Chem. – Eur. J.*, 2000, **6**, 1483–1495.
12 B. Lingen, J. Grötzinger, D. Kolter, M.-R. Kula and M. Pohl, *Protein Eng.*, 2002, **15**, 585–593.
13 P. Domínguez de María, T. Stillger, M. Pohl, M. Kiesel, A. Liese, H. Gröger and H. Trauthwein, *Adv. Synth. Catal.*, 2008, **350**, 165–173.
14 M. Berheide, S. Kara and A. Liese, *Catal. Sci. Technol.*, 2015, **5**, 2418–2426.
15 A. V. Presečki, L. Pintarić, A. Švarc and Đ. Vasić-Rački, *Bioprocess Biosyst. Eng.*, 2018, **41**, 793–802.
16 O. P. Ward and A. Singh, *Curr. Opin. Biotechnol.*, 2000, **11**, 520–526.
17 J. Wachtmeister, A. Jakoblinnert and D. Rother, *Org. Process Res. Dev.*, 2016, **20**, 1744–1753.
18 T. Yamane, *Biocatalysis*, 1988, **2**, 1–9.
19 V. Erdmann, U. Mackfeld, D. Rother and A. Jakoblinnert, *J. Biotechnol.*, 2014, **191**, 106–112.
20 A. Jakoblinnert, R. Mladenov, A. Paul, F. Sibilla, U. Schwaneberg, M. B. Ansorge-Schumacher and P. Domínguez de María, *Chem. Commun.*, 2011, **47**, 12230.
21 J. Wachtmeister and D. Rother, *Curr. Opin. Biotechnol.*, 2016, **42**, 169–177.
22 G. Goetz, P. Iwan, B. Hauer, M. Breuer and M. Pohl, *Biotechnol. Bioeng.*, 2001, **74**, 317–325.
23 H. Bisswanger, *Enzyme Kinetics*, WHILEY-VCH Verlag GmbH, Weinheim, 1st edn, 2002.
24 B. U. Kragl, D. Gygax, O. Ghisalba and C. Wandrey, *Angew. Chem., Int. Ed. Engl.*, 1991, **101**, 827–828.
25 J. Wachtmeister, P. Mennicken, A. Hunold and D. Rother, *ChemCatChem*, 2016, **8**, 607–614.
26 M. Zavrel, T. Schmidt, C. Michalik, M. Ansorge-Schumacher, W. Marquardt, J. Büchs and A. C. Spiess, *Biotechnol. Bioeng.*, 2008, **101**(1), 27–38.
27 E. S. Polovnikova, M. J. McLeish, E. A. Sergienko, J. T. Burgner, N. L. Anderson, A. K. Bera, F. Jordan, G. L. Kenyon and M. S. Hasson, *Biochemistry*, 2003, **42**, 1820–1830.
28 R. W. Lencki, J. Arul and R. J. Neufeld, *Biotechnol. Bioeng.*, 1992, **40**, 1421–1426.
29 F. C. Neidhardt, K. Tummler and R. Milo, *Cell biology by the numbers*, Taylor & Francis, New York, 1990.
30 R. Milo, Overall macromolecular composition of *E. coli* cell.
31 M. S. Hasson, A. Muscate, M. J. McLeish, L. S. Polovnikova, J. A. Gerlt, G. L. Kenyon, G. A. Petsko and D. Ringe, *Biochemistry*, 1998, **37**, 9918–9930.
32 J. Döbber, T. Gerlach, H. Offermann, D. Rother and M. Pohl, *Green Chem.*, 2018, **20**, 544–552.
33 F. H. Andrews and M. J. McLeish, *FEBS J.*, 2013, **280**, 6395–6411.
34 M. Hönig, P. Sondermann, N. J. Turner and E. M. Carreira, *Angew. Chem., Int. Ed.*, 2017, **56**, 8942–8973.
35 B. Mojsoska, G. Carretero, S. Larsen, R. V. Mateiu and H. Jenssen, *Sci. Rep.*, 2017, **7**, 42332.
36 A. F. Makarchikov, B. Lakaye, I. E. Gulyai, J. Czerniecki, B. Coumans, P. Wins, T. Grisar and L. Bettendorff, *Cell. Mol. Life Sci.*, 2003, **60**, 1477–1488.
37 M. Zampieri, K. Sekar, N. Zamboni and U. Sauer, *Curr. Opin. Chem. Biol.*, 2017, **36**, 15–23.

38 M. Oldiges, S. Noack and N. Paczia, Metabolomics in Biotechnology (Microbial Metabolomics), *Metabolomics in Practice*, 2013, pp. 379–391.
39 N. N. Rao, S. Lütz, K. Würges and D. Minör, *Org. Process Res. Dev.*, 2009, **13**, 607–616.
40 A. Liese, K. Seelbach and C. Wandrey, *Industrial Biotransformation*, Wiley-VCH Verlag GmbH & Co. KGaA, Weinheim, 2nd edn, 2006.
41 P. Tufvesson, J. Lima-Ramos, M. Nordblad and J. M. Woodley, *Org. Process Res. Dev.*, 2011, **15**, 266–274.